# Comparison between Analytic Calculation and Finite Element Modeling in the Study of Winding Geometry Effect on Copper Losses

Moustafa Al Eit, Frédéric Bouillault, Guillaume Krebs, Claude Marchand

# Comparison between Analytic Calculation and Finite Element Modeling in the Study of Winding Geometry Effect on Copper Losses

M. Al Eit, F. Bouillault, C. Marchand, and G. Krebs

GeePs | Group of electrical engineering - Paris, UMR CNRS 8507, CentraleSupélec,
Univ. Paris-Sud, Université Paris-Saclay, Sorbonne Universités, UPMC Univ Paris 06
3 & 11 rue Joliot-Curie, Plateau de Moulon 91192 Gif-sur-Yvette CEDEX, France
moustafa.aleit@gmail.com

**The selection of the optimal winding geometry in order to improve the efficiency in electric machines derives from the fact that the level of eddy current losses in machine windings is strongly correlated to the manner of disposition of coil conductors in machine slots. To compute the additional eddy current losses which are part of the total copper losses in the slot windings of electric machines, finite-element modeling is often used; it usually employs moving band technique to perform the rotor motion and Newton-Raphson iterations to deal with the non-linear behavior of magnetic circuits. Finite-element modeling leads then to a substantial computational time which hinders any process of conception and optimization of winding geometries. As an alternative, the analytic calculation that incorporates several simplification hypotheses is investigated. Even though, it is less accurate with regard to the finite-element approach, it presents a first suggestion to select the optimal winding configuration. It is very fast and shows therefore clear interests in repetitive analyses.**

***Index Terms*— Finite element analysis, eddy currents, analytic calculation, switched reluctance machine.**

## I. Introduction

The copper losses are subdivided into classical ohmic dc losses and additional eddy current losses. The latter exists due to the strong electromagnetic coupling between the current density and the time varying magnetic fields penetrating the copper conductors. Due to the fact that this interaction between electric and magnetic variables cannot be solved easily, then the finite-element (FE) method can be used to give a numerical solution [1]. Based on the assumption that the amount of eddy current losses is strongly correlated to the manner of disposition of coil conductors in machine slots, it is firmly recommended to select the optimal winding geometry configuration in terms of copper losses [1,2]. In case of electric machines, FE modeling includes usually the moving band technique to perform the rotor motion and employs the Newton-Raphson iterations to consider the non-linearity of magnetic circuits. Therefore, the choice of the optimized winding configuration using the FE resolution leads to a substantial calculation time and requires large storage capacity. To tackle this issue, the analytic calculation is suggested as an alternative mean [3,4]. Based on several simplification hypotheses, it allows fast and approximate calculation of the copper losses in the slot windings. The switched reluctance machine (SRM) wounded with different winding geometry configurations is taken as an application example where the results concerning the amount of copper losses from the FE modeling and the analytic calculation approach are compared. This type of machine can be used in hybrid or electric vehicle where, for autonomy considerations, energy efficiency is crucial [5].

## II. FE Method Formulation

At low frequencies the displacement currents are neglected, and then the concerned Maxwell's equations in an electromagnetic domain Ω of boundary Γ (Fig. 1) ($\Gamma = \Gamma_1 \cup \Gamma_2$ and $\Gamma_1 \cap \Gamma_2 = 0$) and the associated constitutive medium relationships are given by:

$$\overrightarrow{curl}(\vec{H}) = \vec{J},\ div(\vec{B}) = 0,\ \overrightarrow{curl}(\vec{E}) = -\partial\vec{B}/\partial t \quad \text{(1 a-b-c)}$$

$$\vec{H} = \nu(|\vec{B}|)\vec{B},\ \vec{J} = \sigma\vec{E} \quad \text{(2 a-b)}$$

Where $\vec{B}$ the magnetic flux density vector, $\vec{H}$ the magnetic field vector, $\vec{E}$ the electric field vector and $\vec{J}$ the current density vector. $\sigma$ is the conductivity and $\nu$ the reluctivity. $\nu$ may depend on $B$ in case of ferromagnetic materials with a non-linear behavior. $\nu_0$ is the constant reluctivity of the air. To impose the uniqueness of the solution, boundary conditions must be considered such that:

$$\vec{H} \times \vec{n} = \vec{0} \ \text{ on } \Gamma_1; \qquad \vec{B}.\vec{n} = 0 \text{ on } \Gamma_2 \quad (3)$$

With $\vec{n}$ the outward boundary unit normal vector.

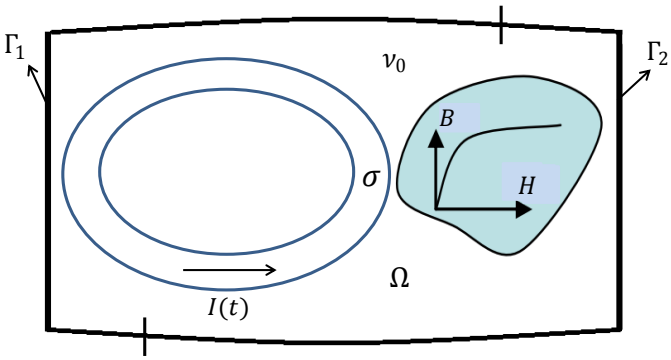


Fig. 1. NL electromagnetic problem coupled with electric circuits

An easy coupling with the electric circuits leads to use in a privileged way the potentials for example the magnetic vector potential $\vec{A}$ defined as $\vec{B} = \overrightarrow{curl}(\vec{A})$ and the electric scalar potential $V$ with $\vec{E} = -\partial\vec{A}/\partial t - \overrightarrow{grad}(V)$. The resultant vector potential formulation from (1) and (2) is given by:

$$\overrightarrow{curl}\left(\nu\overrightarrow{curl}(\vec{A})\right) = -\sigma\partial\vec{A}/\partial t - \sigma\overrightarrow{grad}(V) \quad (4)$$

To impose the current $I(t)$ feeding the conductor of cross section $S$, the following relation must be considered:

$$I(t) = \iint_S \vec{j}.\overrightarrow{ds} = \iint_S \left(-\sigma\partial\vec{A}/\partial t - \sigma\overrightarrow{grad}(V)\right).\overrightarrow{ds} \quad (5)$$

The 2D FE formulation of (4), as well as considering the circuit equation (5) and the backward Euler method for time discretization, leads to the following matrix system [1,6]:

$$\begin{pmatrix} [S] + \frac{[T]}{\Delta t} & [D] \\ [D]^t & \Delta t[G] \end{pmatrix} \begin{bmatrix} [A_t] \\ [\Delta V_t] \end{bmatrix} = \begin{bmatrix} \frac{[T]}{\Delta t}[A_{t-\Delta t}] \\ \Delta t[I(t)] + [D]^t[A_{t-\Delta t}] \end{bmatrix} \quad (6)$$

At instant $t$, $\Delta V_t$ is the electric potential drop (voltage) per unit length. We talk about vectors $[\Delta V_t]$ and $[I(t)]$ of size $N_c \times 1$ each if we consider the case of $N_c$ conductors ($N_c > 1$). $[A_t]$ consists of the set of nodal magnetic vector potential unknowns of size $N_n \times 1$ where $N_n$ the total number of mesh nodes. $[D]$ and $[G]$ are the matrices corresponding to electric circuits and $[T]$ is the singular conductivity matrix. The curl-curl reluctance matrix that accounts for magnetic saturation effects must be written as $[S] = [S(A)]$ in non-linear problems where the Newton-Raphson solver is used in order to converge toward the appropriate solution. In the case of electric machines, the moving band technique is usually adopted to perform the rotor motion.

## III. Analytic Copper Losses Calculation

We consider the case of $n$ individual conductors, placed one on the top of the other in a symmetric slot with parallel edges (Fig. 2). Each of the conductors is fed by the imposed current $I(t)$. We start from the assumptions that the permeability of the iron is very high then the magnetic field in the lamination material is negligible. We add the hypotheses such as the magnetic and electric fields are independent of $x$ and $z$ and that each of them has one component in the $x$ direction for the magnetic field $H(y) = H_x(y)$ and in the $z$ direction for the electric field $E(y) = E_z(y)$ [3]. In the copper conductors the current density is given by $J(y) = J_z(y) = \sigma E(y)$.

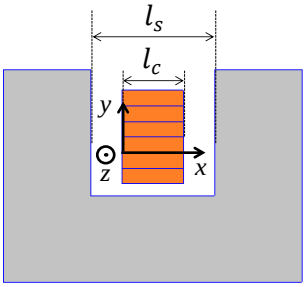


Fig. 2. Example of $n$=6 conductors in a symmetrical slot with parallel edges

Applying Ampere's law and Faraday's law to a conductor section of height $dy$, length $l$ along z-axis and width $l_c$ placed in a slot of width $l_s$, results in the following differential equations of $H(y)$ and $E(y)$:

$$\frac{d(H(y))}{dy} = \frac{\sigma l_c}{l_s}E(y) \quad (7)$$

$$\frac{d(E(y))}{dy} = \mu\partial H(y)/\partial t \quad (8)$$

Where $\mu$ and $\sigma$ are the copper permeability and conductivity respectively. Equations (7) and (8) are understood as the fundamental equations for the analytic calculation of the ac copper losses [3,4]. $l_c/l_s$ is called the Dowell's layer copper factor. We must emphasize the fact that the validity of the analytic loss calculation decreases when the Dowell's layer copper factor becomes small i.e. the copper width $l_c$ becomes small compared to the slot width $l_s$ [7]. Assuming sinusoidal quantities, the current $I(t)$ given by the expression $I(t) = I\sqrt{2}sin(wt + \varphi)$, will have the well-known complex representation $\underline{I} = Ie^{j\varphi}$ where $I$ is the *rms* value, $w$ the angular frequency and $\varphi$ the phase at the origin of time. Then, the electric and magnetic fields and the current density can be written with their corresponding complex notations $\underline{E}(y)$, $\underline{H}(y)$ and $\underline{J}(y)$ respectively. Combining now equations (7) and (8) in their complex forms yields a second order differential equation:

$$\frac{d^2(\underline{H}(y))}{dy^2} - j\omega\mu\frac{\sigma l_c}{l_s}\underline{H}(y) = 0 \quad (9)$$

with the solving approach:

$$\underline{H}(y) = c_1e^{ry} + c_2e^{-ry} \quad (10)$$

Where $c_1$ and $c_2$ are the complex constants and $r$ is given by the following expression:

$$r = \sqrt{j\omega\mu\sigma l_c/l_s} \quad (11)$$

Since the electric field and consequently the current density are not continuous at the edge of the conductors, the expressions of the magnetic and electric fields are determined for each conductor separately. The origin of the coordinate system is considered located at the lower edge of the regarded conductor (Fig. 2). To determine the constants $c_1$ and $c_2$, the boundary conditions of the magnetic field $\underline{H}(0)$ at the lower edge and $\underline{H}(h)$ at the upper edge of the regarded conductor can be utilized. Where $h$ is the height of the individual conductor. A parameter $p$ identifies the conductor within the slot with $1 \le p \le n$, where $n$ is the total number of slot conductors placed on top of each other. The line of magnetic flux passing through the lower edge of the conductor $p$ at $y$=0 surrounds $(p\text{-}1)$ times the current $\underline{I}$ and that passing through the upper edge at $y$=$h$ surrounds $p$ times the current $\underline{I}$. Using the equation (10), these two boundary conditions yield the following two equations with which the complex constants $c_1$ and $c_2$ can be determined:

$$(c_1 + c_2)l_s = (p-1)\underline{I} \quad (12)$$

$$(c_1 e^{rh} + c_2 e^{-rh}) l_s = p\underline{I} \tag{13}$$

Determining $c_1$ and $c_2$ gives the magnetic field distribution along the regarded conductor $p$:

$$\underline{H}(y) = \frac{\underline{I}}{l_s \sinh(rh)} [p \sinh(ry) - (p-1)\sinh\big(r(y-h)\big)] \tag{14}$$

From (14) the expression of the electric field can be deduced using the equation (7). By multiplying the electric field by $\sigma$, the current density valid for conductor $p$ is calculated to:

$$\underline{J}(y) = \frac{r\underline{I}}{l_c \sinh(rh)} [p \cosh(ry) - (p-1)\cosh\big(r(y-h)\big)] \tag{15}$$

The total copper losses of conductor $p$ can be calculated according to the following equation:

$$P = l_c l/\sigma \int_0^h \left|\underline{J}(y)\right|^2 dy \tag{16}$$

To calculate the absolute value of $\underline{J}(y)$, the hyperbolic functions have to be split into their real and imaginary parts, then the total copper losses of the conductor $p$ can be written as :

$$P_{ACp} = R_{DCp} I^2 [\varphi(x) + p(p-1)\psi(x)];\ x = hr/\sqrt{2j} \tag{17}$$

with

$$R_{DCp} = \frac{l}{\sigma h l_c} \tag{18}$$

The corresponding functions $\varphi(x)$ and $\psi(x)$ are:

$$\varphi(x) = x \frac{(\sinh 2x + sin2x)}{\cosh 2x - \cos 2x} \tag{19}$$

$$\psi(x) = 2x \frac{(\sinh x - sinx)}{\cosh x + \cos x} \tag{20}$$

The function $\varphi(x)$ is referred to as the skin effect factor while $\psi(x)$ is called proximity effect factor. To calculate now the total losses of the $n$ slot conductors, the individual conductor losses $P_{ACp}$ have to be summed up which leads to the following expression of the total copper losses:

$$P_{AC} = \sum_{p=1}^{n} P_{ACp} = R_{DC} I^2 \left[\varphi(x) + \frac{(n^2-1)}{3}\psi(x)\right] \tag{21}$$

with, $R_{DC}$ the total dc resistance of the $n$ slot conductors, $R_{DC} = nR_{DCp}$.

In case of periodic non sinusoidal current waveforms, the total copper losses can be calculated by summing the losses corresponding to all Fourier spectral components [4,8]. The periodic feeding current $I(t)$ of frequency $w/2\pi$ may be represented by its Fourier series expansion:

$$I(t) = I_{DC} + \sum_{k=1}^{\infty} I_k \sqrt{2} \sin(kwt + \varphi_k) \tag{22}$$

Where $I_{DC}$ is the dc value of $I(t)$, $I_k$ is the rms value of the *kth* harmonic with corresponding phase $\varphi_k$. The total copper losses due to all the harmonics is then:

$$P_{AC} = R_{DC}[I_{DC}^2 + \sum_{k=1}^{\infty} I_k^2 \left[\varphi(x_k) + \frac{(n^2-1)}{3}\psi(x_k)\right]] \tag{23}$$

The skin and proximity effect factors have to be determined separately evaluating equations (19) and (20) with:

$$x_k = hr_k/\sqrt{2j} \text{ and } r_k = \sqrt{jk\omega\mu\sigma l_c/l_s} \tag{24}$$

## IV. Application Examples

We start the study of two test case examples. The first one is a skin effect example, it is about one conductor ($n$=1) (Fig. 3) of cross section $S$ placed in a symmetric slot with parallel edges and fed by the current $I(t)$. The second is a proximity effect example, it is about 18 conductors (3x6) fed each one by the current $I(t)$/18 (Fig. 3). (3x6) configuration means that we have three horizontal layers with 6 vertical conductors by layer. Each conductor has a cross section of $S$/18. First, the FE modeling is implemented. In Figure 4, the copper losses in skin and proximity effect examples and their common dc losses are plotted in function of time. Both winding configurations are fed by the same typical SRM magnetomotive force (MMF) waveform $I(t)$ at the frequency of 1000 Hz (Fig. 4). It is a non-sinusoidal waveform whose ten first Fourier spectral components are shown in figure 5.

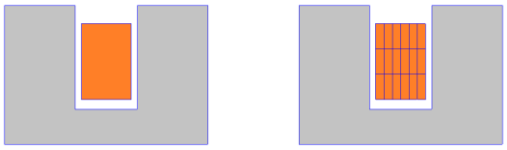

Fig. 3. Left: Skin effect example . Right: Proximity effect example.

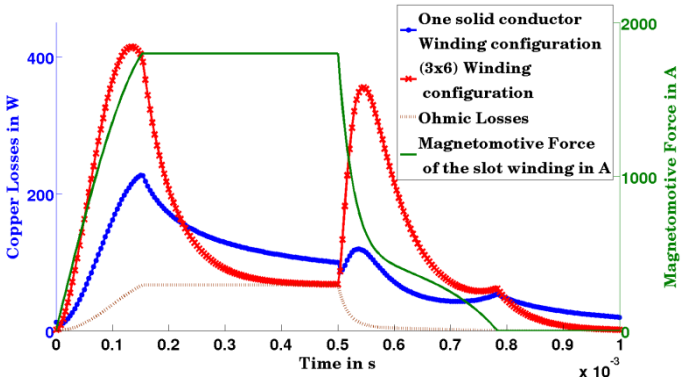


Fig. 4. Copper losses calculated by the FE modeling in both skin and proximity effect examples.

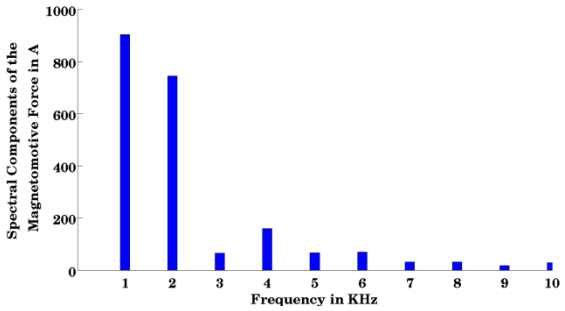


Fig. 5. Fourier coefficients of the MMF of the slot winding

The presented equation (23) for analytic calculation of the copper losses occurring in a slot segment of length $l$ and width $l_s$ is defined for winding geometries which have the total width $l_c$ and covers $n$ horizontal conductors of height $h$.To calculate the losses of a given winding in a given parallel slot edges, these five geometric parameters $l$, $l_s$, $l_c$, $n$ and $h$ are fundamentals. For a given winding topology, the number of winding layers $n$ has to be determined by transforming the investigated winding geometry configuration into an equivalent geometry. Depending on the real winding geometry, usually numerous winding turns are merged during this process in a way that the total MMF of the original and the equivalent geometry are equal. In the one hand, for the skin effect example, no winding transformation is needed, the number of winding layers is $n$=1. In the other hand, figure 6 illustrates the geometry adaptation for the studied (3x6) winding configuration. Due to symmetry reasons, the current distribution inside the six conductors of each horizontal layer must be equal since all conductors are fed by the same current and are penetrated by the same magnetic field $H_x(y)$. Hence, the six conductors can be merged into one solid conductor fed by the current $I(t)/3$. The proximity effect example is then about a three-layer winding ($n$=3) (Fig. 6).

Fig. 6. Determination of the equivalent winding geometry when the six turns of each winding layer can be merged into one solid conductor

When all geometric parameters of both examples are determined, the analytic calculation can be carried out. Although the chosen conductor dimensions and the excitation frequency do not match realistic conditions for a slot winding application, the examples illustrate the strong influence of the winding configuration on the ac losses. Both configurations have the same dc resistance and produce the same amount of MMF but still the ac losses of the second example are about 1.5 times higher than those of the first example. The copper losses calculated by the FE simulations are very close to analytic values with an error that does not exceed the 3.2% (Table 1).

An SRM 8/6 is taken now as a more realistic example. Only one phase is fed, it consists of two coils connected in series; each of them has 18 turns. Half of the machine is studied for periodic reasons (Fig. 7). The 18 coil turns can be distributed in machine slots in different ways which leads to various winding configurations. The coil conductors can be placed horizontally (18x1), vertically (1x18) or as other different configurations such as (9x2), (6x3), (3x6) or (2x9) (Fig. 8). Based on the assumption that the amount of eddy current losses is strongly correlated to the manner of disposition of coils in machine slots, it is firmly recommended to select the optimal winding configuration in terms of copper losses.

Table 1. Comparison between the loss calculation methods for the examined test case examples.

| Test Case | Copper Losses in W | | Ohmic Losses in W |
|---|---|---|---|
| | Analytic Calculation | FE Model | |
| Example 1 ($n$=1) | 87.81 | 89.43 | 29.18 |
| Example 2 ($n$=3) | 131.92 | 127.72 | |

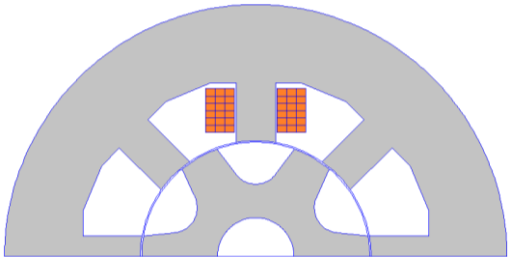

Fig. 7. SRM with a 18 turns coil ((6x3) winding configuration)

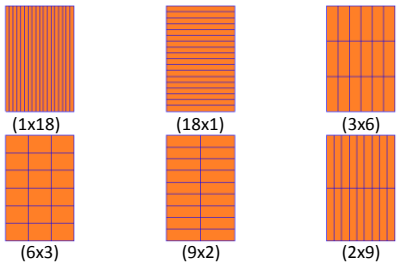


Fig. 8. Different winding geometry configurations in the case of 18 turn conductors

First, the copper losses are calculated for the different winding geometry configurations using the FE modeling. Then, the analytic loss calculations are carried out. However, several parameters $l$, $l_s$, $l_c$, $h$ and $n$ have to be determined first of all.

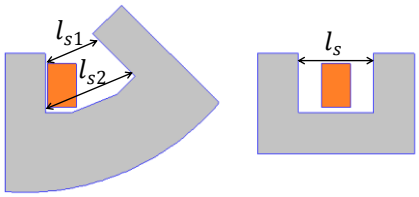


Fig. 9. Left: The real slot geometry of the SRM, Right:the equivalent slot geometry.

The real slot geometry of the electric machine is transformed into an equivalent geometry which then allows the extraction of the geometric parameters. Since the slot edges in SRM are not parallel, it seems reasonable to calculate a mean value for $l_s$ with the equation (25) in which $l_{s1}$ and $l_{s2}$ are the slot width at the upper and the lower edge of the coil slot winding (Fig. 9).

$$l_s = \frac{l_{s1} + l_{s2}}{2} \tag{25}$$

The equivalent slot geometry is a symmetric slot with parallel edges; we come across the slot geometry that was studied

in the test case example. Then, to determine the number of winding layers $n$, all real winding configurations are transformed into their corresponding equivalent geometries following the same principle that was shown in Figure 6. The analytic calculation in case of sinusoidal currents shows the clear correlation between the copper losses and the winding geometry configurations (Fig. 10). Now, two real operating points at speeds 1100 and 5000 rev/min are studied (Table 2). The control parameters of the current supply are precalculated by the homemade tool MRVSIM [9]. At constant speed, the rotor position is proportional to time. The current waveforms for both operating points are plotted in Figure 11 as function of rotor position, because electrical degrees are more intuitive than a time scale. The origin of the position axis in Figure 11 presents the unaligned position where the stator pole corresponding to the excited phase is equidistant from the adjacent two rotor poles as shown in Figure 7. The rotation from one unaligned position to the consecutive one corresponds to a total of 360 electrical degrees. The turn on angle $\theta_{on}$ declares the magnetization of the phase with respect to the unaligned position. With increasing speed, $\theta_{on}$ has to be advanced and the current waveform changes from a square to a single pulse waveform [5]. The turn on angles for the first and the second operating points are respectively $\theta_{on1} = -50.3°$ and $\theta_{on2} = -97.47°$ (Fig. 11).

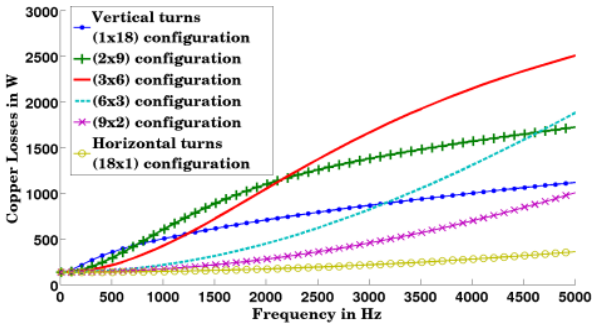


Fig. 10. Correlation between the copper losses and the winding configurations

At the relatively low speed 1100 rev/min corresponding to the first operating point, FE modeling and the analytic calculation results are in agreement; they show that the vertical turns (1x18) configuration is the worst winding configuration producing the highest amount of copper losses while the (9x2) or the (18x1) configurations are the optimal choices. In case of the high speed 5000 rev/min corresponding to the second operating point, the concordant results of the FE modeling and the analytic calculation underline that one of the configurations (9x2) or (18x1) seems to be also the optimal choice since they lead to the lowest amount of copper losses (Table 2). Analytic calculation insures very fast calculation and presents an accepted first suggestion to select the optimal winding geometry configuration. Even if it does not give very close copper loss values to those calculated by the FE method, it can be used as an efficient mean to study the winding configuration influence on the copper losses for a given range of operating frequencies. The non matching values of copper losses given by analytic and FE calculations are expected since the non linearity of the magnetic circuits and the effect of the rotor motion are neglected in the analytic calculations. Adding to the foregoing, the simplifications in winding and slot geometries and the hypothesis that we have assumed regarding the one-dimensional representation of electric and magnetic fields.

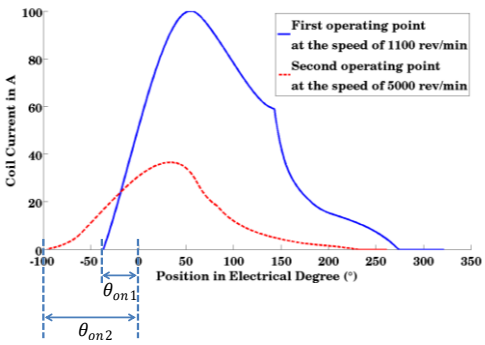


Fig. 11. The current waveforms of the 1st and the 2nd operating points of the SRM

Table 2. Comparison between the mean copper losses calculated by the analytic approach and the FE modeling for the multiple winding configurations and the both operating points of the SRM

| **Configuration Type** | **Copper Losses in W** | | | |
|---|---|---|---|---|
| | **Operating point 1** | | **Operating point 2** | |
| | **Analytic** | **FE** | **Analytic** | **FE** |
| (1x18) | 84.97 | 95.07 | 16.09 | 20.44 |
| (2x9) | 79.91 | 85.28 | 14.72 | 22.24 |
| (3x6) | 78.3 | 81.13 | 11.94 | 18 |
| (6x3) | 77.3 | 78.31 | 9.51 | 11.98 |
| (9x2) | 77.02 | 77.99 | 9.01 | 10.95 |
| (18x1) | 77.14 | 78.88 | 8.7 | 11.43 |
| **Ohmic Losses in W** | 76.9 | | 8.6 | |

## V. Conclusion

Starting from several simplifying assumptions, the analytic model allows very fast calculation of winding copper losses and presents a first suggestion to select the optimal winding geometry configuration. As a coarse model, it may be associated with the fine FE model in optimization methodologies such as the output space mapping technique.

## VI. References


[1] M. Al Eit *et al.*, "2D Reduced Model for eddy currents calculation in Litz Wire and Its Application for Switched Reluctance Machine", IEEE Trans. Magn., vol. 52(3), Oct. 2015.

[2] M. Klauz and D.G. Dorrell, "Eddy current effects in a switched reluctance motor", IEEE Trans. Magn., vol. 42(10), pp. 3437-3439, Oct. 2006.

[3] P. L. Dowell, "Effect of eddy currents in transformer windings", IEE Proc., vol. 113(8), pp. 1387–1394, Aug. 1966.

[4] W. Hurley, E. Gath, and J. Breslin, "Optimizing the ac resistance of multilayer transformer windings with arbitrary current waveforms", IEEE Transactions on Power Electronics, vol. 15(2), pp. 369-76, Mar. 2000.

[5] H. Hannoun, M. Hilairet, C. Marchand, "Design of an SRM Speed Control Strategy for a Wide Range of Operating Speeds", IEEE Trans. on Industrial Electronics, vol. 57(9), pp. 2911-2921, Sept. 2010.

[6] F. Piriou and A. Razek, "Coupling of saturated electromagnetic systems to non-linear power electronic device", IEEE Trans. Magn., vol. 24(1), pp. 274-277, Jan. 1988.

[7] F. Robert, "Eddy current losses: A theoretical discussion of Dowell\'s layer copper factor", *EPE J.*, vol. 12(3), pp. 9-15, 2002.

[8] P.S. Venkatraman, "Winding Eddy Current Losses in Switch Mode Power Transformers Due to Rectangular Wave Currents", Proceedings of Powercon 11, Power Concepts Inc., Venturs, California, 1984, Section A-I, pp. 1-11.

[9] M. Besbes and B. Multon, "MRVSIM logiciel de simulation et d'aide à la conception de machines à réluctance variable à double saillance à alimentation électronique Deposit APP CNRS, Patent IDDN.FR.001.430010.000.S.C.2004.000.30645", 2004.